

Monte Carlo and Modified Tanford–Kirkwood Results for Macromolecular Electrostatics Calculations

Sidney Jurado de Carvalho,[†] Renato Carlos Tonin Ghiotto,[‡] and Fernando Luís Barroso da Silva^{*,§}

Departamento de Física, Instituto de Biociências, Letras e Ciências Extras, Universidade Estadual Paulista, 15054-000 – Rua Cristovão Colombo, 2265, Jd. Nazareth, São José do Rio Preto, SP, Brazil, Departamento de Física, Faculdade de Ciências, Universidade Estadual Paulista, Av. Eng. Luiz Edmundo Carrijo Coube, s/n – Vargem Limpa, 17033-360, Bauru, SP, Brazil, and Departamento de Física e Química, Faculdade de Ciências Farmacêuticas de Ribeirão Preto, Av. do café, s/no., Universidade de São Paulo, 14040-903 Ribeirão Preto, SP, Brazil

Received: August 29, 2005; In Final Form: January 30, 2006

The understanding of electrostatic interactions is an essential aspect of the complex correlation between structure and function of biological macromolecules. It is also important in protein engineering and design. Theoretical studies of such interactions are predominantly done within the framework of Debye–Hückel theory. A classical example is the Tanford–Kirkwood (TK) model. Besides other limitations, this model assumes an infinitesimally small macromolecule concentration. By comparison to Monte Carlo (MC) simulations, it is shown that TK predictions for the shifts in ion binding constants upon addition of salt become less reliable even at moderately macromolecular concentrations. A simple modification based on colloidal literature is suggested to the TK scheme. The modified TK models suggested here satisfactorily predict MC and experimental shifts in the calcium binding constant as a function of protein concentration for the calbindin D_{9k} mutant and calmodulin.

Introduction

It is often demonstrated that electrostatic interactions are crucial for the complex correlation between structure and function of biological macromolecules.^{1–8} There is also evidence that the understanding of biomolecular electrostatics properties can guide protein engineering and design.^{5,9–12} This is quite natural since most such molecules carry ionizable groups in aqueous solutions, and there is a clear relation of dependency between ionic strength, pH, the stability, and the function of proteins.^{3,13–15} A classical example is human hemoglobin, which is regulated physiologically by salt ions and protons.¹⁶ Furthermore, the binding of charged ligands (a proton, a metal ion, a charged substrate, a polyelectrolyte, or another macromolecule) to biomolecules is largely driven by electrostatic forces.^{17–23}

Besides the well-known salt electrostatic screening effect, it has been observed that other important mechanisms can shield electrostatic interactions. Different experiments^{17,18,22,24} have shown that electrostatic interactions can be modulated by *all* charged species in the surrounding solution and not just by the addition of salt ions.

In the complex in vivo conditions there is a large number of charged species (e.g., DNA, several proteins, etc.)^{19,25} in different concentrations that all can interfere in their intermolecular interactions. By mimicking this biological environment by simplified systems, we investigated the binding of barium ions to the chelator 5,5'-Br₂BAPTA [5,5'-dibromo-1,2-bis(*O*-aminophenoxy)ethane-*N,N,N',N'*-tetraacetic acid] in the presence of charged species.²² Several experimental conditions were compared, and it was shown that the binding can be affected in an

anomalous way by the presence of silica sol particles; the added salt *increased* the binding due to the presence of another charged species (in this case, the inert silica sol particles that only electrostatically interfere in the system). Monte Carlo simulations have reproduced the same experimental behavior using a purely electrostatic model.²² These findings emphasize the fact that the macromolecular charge, the number of all charged species present in the system, and their concentrations have to be included for a proper description of the shielding phenomena. The protein concentration effect is particularly important because some proteins inside a biological cell can be found in macromolecular concentrations on the order of millimolar.²⁶ Moreover, in NMR studies of proteins the typical protein concentration is on the order of 1 mM,²⁷ and the concentration of the accompanying counterions could be an order of magnitude larger or more.¹⁸

The theoretical study of biomolecular electrostatics problems has involved extensively the Debye–Hückel (DH) theory.²⁸ Since its first application by Linderstrøm–Lang to the protein titration problem,²⁹ it still serves as the basis for many modern calculations.^{7,30–34} Even despite the advent of fast computers and the possibility to solve the nonlinear Poisson–Boltzmann (NLPB) theory numerically for arbitrary macromolecular shapes,³⁵ many works today routinely assume its linear approximation to describe electrostatic interactions in biochemical systems,^{7,30–33} which is equivalent to treating the system on the DH level. A distinguishable similar scheme is the Tanford–Kirkwood (TK) model.³⁶ This classical analytical model is also based on the same DH framework and as such neglects explicit ion–ion interactions and nonlinear thermal effects. A further simplification is that in all these approaches the macromolecular concentration (c_p) is not even defined. Therefore, this is equivalent to assuming an infinite dilution regime ($c_p \rightarrow 0$) and would limit their application to describe a more general screening phenomena where all charged species do contribute since they were not designed to treat this kind of effect.

* Author to whom correspondence should be addressed. Phone: +55 (16)3602-4219. Fax: +55 (16)3633-2960. E-mail: fernando@fcfrp.usp.br.

[†] Universidade Estadual Paulista, São José do Rio Preto.

[‡] Universidade Estadual Paulista, Bauru.

[§] Universidade de São Paulo.

In principle, the complete screening phenomena can be totally described by explicit solute particle models solved via numerical simulations using either Monte Carlo or molecular dynamics calculations.^{17,37–40} This is also an alternative to replace the mean-field procedures (DH, NLPB, and TK) and the approximate numerical solutions that they provide by *exact* solutions (within statistical errors) for a given effective Hamiltonian. The unfavorable issue is that the computational costs might be higher for these non-mean-field approaches (or even prohibitive at high ionic strengths and moderate macromolecular concentrations), which is not always convenient principally in some more specific applications where there is a need for very fast calculations. This is the case, for instance, if one intends to facilitate the application of electrostatic calculations for protein structure prediction and homology modeling.⁴¹ In an analogous way, less expensive procedures might also be decisive when used to filter a set of designed molecules by combinatorial chemistry, discarding unsuitable ones for the pharmaceutical industry. In this context, the TK model is appealing in that rather cheap calculations can be performed. Furthermore, besides a few significant limitations,² this description was found to be a reasonably good approximation for studies of the binding of spherical ligands to moderately charged macromolecules at low protein concentrations.²⁰ However, it is clear that increasing the macromolecular concentration pushes the TK description to become less reliable. This is also true for the DH and NLPB schemes that are widely used by classical numerical PB solver protocols such as DelPhi,⁴² MEAD,⁴³ and UHBD.⁴⁴ Hence, one important information is to clarify when it would not work.

The purpose of the present work is twofold: The first effort here is to evaluate the protein concentration screening effect as described by the mean-field approaches. The TK scheme will be tested for the sake of convenience. By using Monte Carlo (MC) simulations to resolve the effective Hamiltonian, we will determine the validity of both the original TK scheme and the modified versions suggested here. These modifications allow the introduction of the macromolecular concentration parameter in a simple manner in the TK scheme, which enables the reproduction of real experimental data. As a test case, Ca²⁺ binding constants to a mutant calbindin D_{9k} (N56A) and calmodulin¹⁸ are used to benchmark the new method. The second issue is to demonstrate that this macromolecular screening phenomena can also be analytically predicted.

Methods

Model Systems. A great positive step introduced by Tanford and Kirkwood was the possibility to consider all titratable groups to be placed at specific locations in the protein model interior rather than smeared out on the protein surface.³⁶ Therefore, it is with regard to theory perfectly possible to use the crystallographic macromolecular structure (e.g., X-ray coordinates) in the TK description. The proteins were modeled here both as rigid bodies in full atomistic details according to the X-ray structures provided by the Protein Data Bank^{45,46} and as more simplified crude models.

For the sake of simplicity and generality, in the first part of the present study, we will mimic any common globular protein by a rigid sphere with radius R_p and a single central net charge (Z_p)—model 1. Internal structural details of the protein will be initially neglected. Besides different net charges in some cases, the simplified protein models are made as a caricature of the calcium binding protein calbindin D_{9k}⁴⁷ in an attempt to keep our theoretical analysis as close as possible to real biochemical systems without losing the generality. Therefore, they are supposed to simultaneously bind two divalent ions at sites located

at the Cartesian coordinates (7.340, 7.114, −1.607) and (10.503, −3.509, −0.364), in angstroms, assuming the protein center of mass as the origin.²⁰ In a second set of simulations, a more realistic protein model is used. In this case, an all-atom model (model 2) using structural data for calbindin (PDB code 3ICB)⁴⁸ and calmodulin (PDB code 3CLN)⁴⁹ will be employed in the final part of this work as test cases for our general approach.

The protein model in its apo form is immersed in an electrolyte solution described by the so-called restricted primitive model.⁵⁰ This means that each mobile ion (added salt and counterions) is treated as a hard sphere of radius R_k and charge z_k . The solvent only enters through its average dielectric permittivity ϵ_s that is also assigned to the ionic and protein interiors (ϵ_p). The choice of ϵ_p is an issue under intense debate in the literature.^{4,51–58} Many times ϵ_p is arbitrarily chosen without a reasonable physical argument to obtain the best agreement between the predicted electrostatic properties and the experimental results. The assumption of the homogeneous macromolecular dielectric response in this work is based on recent data where it was shown that the presence of a dielectric interface gives unphysical results when used to predict mutational effects on the calcium binding constant to calbindin.^{38,40,59} Moreover, calculations performed with a uniform continuum model as done here successfully reproduced experimental data^{17,22,23,60–62} in contrast with others where a low dielectric response was adopted.^{38,63} Hence, two ionized sites i and j (either a protein fixed charge or a mobile ion) with a spatial separation distance $r_{ij} > R_i + R_j$ contribute to the electrostatic potential energy simply by the ordinary Coulomb potential

$$u^{\text{el}}(r_{ij}) = \frac{z_i z_j e^2}{4\pi\epsilon_0\epsilon_s r_{ij}} \quad (1)$$

where e , ϵ_0 , z_i , and z_j denote the elementary charge, the vacuum permittivity, and the valence of charges i and j , respectively. When $r_{ij} \leq R_i + R_j$, a short-range hard-core overlap restriction among the charges (u^{hs}) is included to prevent the Coulomb collapse

$$u^{\text{hs}}(r_{ij}) = \begin{cases} \infty, & r_{ij} \leq (R_i + R_j) \\ 0, & \text{otherwise} \end{cases} \quad (2)$$

This potential accounts as well for the macromolecular excluded volume.

All of the system—protein, added salt, and counterions—is placed and confined in a spherical cell of radius R_c determined by the macromolecular concentration (c_p); see Figure 1. This is referred to in the literature as the *cell model*.^{28,64,65} That is the manner in which protein–protein interactions are partially taken into account.^{64,66} The R_c values used in this work are shown in Table 1. The cell boundary constraint acting as a hard wall is imposed as an one-body external field $v^{\text{ex}}(r_i)$

$$v^{\text{ex}}(r_i) = \begin{cases} 0, & (R_i + R_p) \leq r_i \leq R_c \\ \infty, & \text{otherwise} \end{cases} \quad (3)$$

When eqs 1–3 are combined, the full configurational energy of the system is defined

$$U(\{\mathbf{r}_k\}) = \sum_{i=1}^{N_c+N_s} v^{\text{ex}}(r_i) + \frac{1}{2} \sum_{i=1}^N \sum_{j=1}^N (u^{\text{el}}(r_{ij}) + u^{\text{hs}}(r_{ij})) \quad (4)$$

where N_c and N_s are the number of mobile counterions and mobile added salt ions, respectively. The total number of charges is $N = N_c + N_s + N_p$ which also comprises the fixed protein

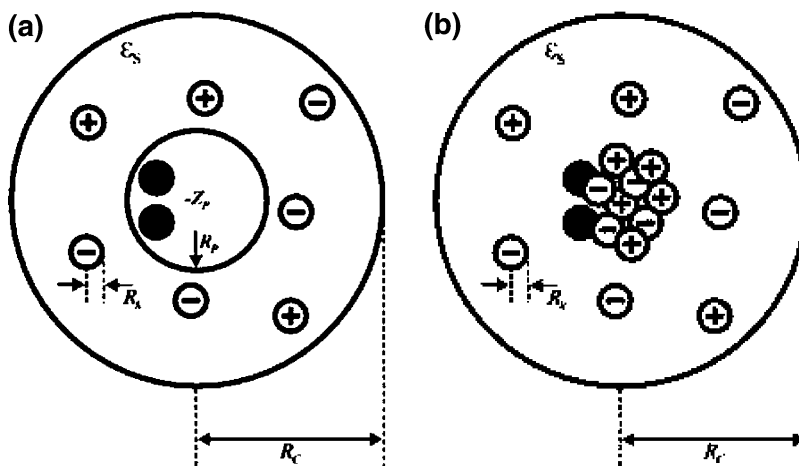


Figure 1. Schematic representation of the model system. (a) A charged spherical protein in a spherical cell with radii R_p and R_c , respectively, is seen surrounded by counterions and added salt particles (radius R_s). The central charge has the valency Z_p . Two binding sites marked with a black dot are also shown. (b) Protein represented by its titratable groups placed in specific locations within a spherical cavity with radius R_p .

TABLE 1: Parameters Used in Our Monte Carlo Simulations

protein concentration (mM)	cell radii (\AA) ^a	salt concentration (mM)	number of positive particles ^b	number of negative particles
0.02	270.63	1	58	50
		2	108	100
		5	258	250
		10	508	500
		25	1258	1250
		50	2508	2500
0.20	125.61	100	5007	4999
		1	13	5
		2	18	10
		5	33	25
		10	58	50
		25	141	133
2.00	58.30	50	258	250
		100	508	500
		1	9	1
		2	9	1
		5	11	3
		10	13	5
		25	21	13
		50	33	25
		100	58	50

^a R_c is given accordingly with the protein concentration. ^b The number of counterions is given here for a protein net charge of $Z_p = -8e$ modeled by model 1.

charges. For all calculations done with model 1, N_p was set equal 1. Conversely, for the calculations done with the all-atom model (model 2), atomic charges were attributed to protein atoms according to Linse et al.,¹⁸ which implies that at pH = 7.5, $N_p = 46$ for calbindin (a moderately charged protein) and $N_p = 107$ for calmodulin (a highly charged protein).

Numerical Simulations. Monte Carlo (MC) simulations performed here in the canonical (NVT) ensemble were primarily used to investigate the TK descriptions. The standard Metropolis algorithm^{40,67} was used to sample equilibrium configurations. In all sets of simulations counterions and monovalent added salt (symmetrical 1:1 electrolyte) with a common radius of $R_k = 2 \text{ \AA}$ for all k were allowed to move through the cell. The macromolecule in either its coarse level (model 1) or all-atom representation (model 2) was kept fixed at the center of the cell. The cell radius was determined straightforwardly by c_p , except when the number of salt ion particles required in the simulation

becomes highly prohibitive. Although a large number of ionic particles were used here (Table 1), typically, 50–100 salt pairs were sufficient to ensure a proper thermodynamical description of the system in the salt and proteins concentration regimes reported in this work.

The salt concentration (c_s) varied from 0 to 1000 mM in our calculations, while c_p was in the range from 0.02 to 7.35 mM. We note here that the choice of the smallest c_p value is based both on typical experimental conditions^{60,68} and on previous theoretical analysis where the TK description is known to perform well, at least, for moderately charged proteins.²⁰ The macromolecule radius was $R_p = 14 \text{ \AA}$, and its net charge (in units of the elementary charge) was varied to correspond to from a weakly to a relatively highly charged protein, i.e., from $Z_p = -4$ to $Z_p = -24$, except for the all-atom model. In this case, a diameter equal to 4 \AA was assigned to each protein atom, and the charge parameters followed the already mentioned criterion.¹⁸ This is a reasonable size, and the results are not sensitive to this particular detail. An appropriate number of monovalent counterions (N_c) was always added to maintain the electroneutrality of the system. As usual, the temperature was fixed at $T = 298.15 \text{ K}$, and the solvent static dielectric constant was taken to be $\epsilon_s = 78.7$.

Free Energy Calculations. The total free energy (ΔG^{tot}) can be partitioned in terms of electrostatic interactions (ΔG^{el}) and all other effects (solvent ordering, protein structural changes, etc.). Assuming that the latter gives a negligible contribution when comparing different salt and/or protein concentration regimes (i.e., ΔpK), one just needs to obtain the ΔG^{el} values from excess chemical potentials (μ^{ex}) that can be calculated as ensemble averages over the unperturbed system. The stoichiometric binding constants (K) were measured in the MC simulations by a perturbation method usually referred to as Widom's test particles technique.^{69,70} Details of this technique have been reported previously.^{17,20,22,60,66,71} From this approach, shifts in ion binding constants upon addition of salt can be calculated as

$$\Delta pK = \beta(\Delta G^{\text{el}} - \Delta G_{\text{ref}}^{\text{el}})/\ln(10) \quad (5)$$

where $\beta = 1/k_B T$, k_B is the Boltzmann constant, and ΔG^{el} can be written in terms of the excess chemical potentials of protein (P), protein + ligand (P + L), and free ions (F). That is

$$\Delta G^{\text{el}} = (\mu_{\text{P+L}}^{\text{ex}} - \mu_{\text{P}}^{\text{ex}}) - \mu_{\text{F}}^{\text{ex}} \quad (6)$$

By application of the insertion procedure, $\mu_{\text{B}}^{\text{ex}} = \mu_{\text{P+L}}^{\text{ex}} - \mu_{\text{P}}^{\text{ex}}$ is

calculated simply by inserting the test particles directly at the binding sites and taking into account the interaction between the two ligands (calcium ions). Random particle insertions over the entire cell give the excess chemical potential of the free ions. An attempt to insert virtual Widom's test particles not affecting the Markov chain was made with a probability of 0.2 during 100 000 simulation cycles of the production phase after a proper equilibration.

The system at $c_s = 1$ mM was chosen as the reference state for each given protein concentration in most of the studied cases. It is at this salt concentration that $\Delta G_{\text{ref}}^{\text{el}}$ was calculated in most of our simulations. The shifts in binding constant as a function of macromolecular concentration were obtained in a similar manner.

Tanford–Kirkwood Analysis. The original Tanford–Kirkwood (TK) model³⁶ has been analyzed in some detail in ref 20. Therefore, it is sufficient to mention here that this description resembles the protein cell model previously described (Figure 1) with further simplifications. Instead of confining the system in a rigid reservoir, it is assumed an infinitesimally small macromolecule concentration and the accompanying counterions are neglected, even when their concentrations might be indispensable. The full statistical mechanical treatment of the mobile ion motion is also avoided by the introduction of the DH potential necessary to calculate the electrostatic contributions to the free energy (G^{el}).³⁶ From TK, the logarithmic change in the stoichiometric binding constant (ΔpK) is given by eq 6. Nevertheless, here $\mu_{\text{F}}^{\text{ex}}$ is analytically calculated from the Debye–Hückel theory of strong electrolytes and reads

$$\beta\mu_{\text{F}}^{\text{ex}} = -\frac{\kappa z^2 e^2}{8\pi\epsilon_0\epsilon_s(1 + 2\kappa R_s)} \quad (7)$$

where $R_s = R_k$ is the mobile added salt radius, z is the valency of the ligand and κ is the inverse DH screening length defined by (for a bulk number density of species k equal to $n_{0,k}$)⁷²

$$\kappa = \left[\frac{e^2}{\epsilon_0\epsilon_s k_B T} \sum_1^N n_{0,k}(z_k)^2 \right]^{1/2} \quad (8)$$

Similarly, the excess chemical potential at the binding site ($\mu_{\text{B}}^{\text{ex}}$) is directly calculated as $\mu_{\text{B}}^{\text{ex}} = G^{\text{el}}(\text{P} + \text{L}) - G^{\text{el}}(\text{P})$. Note that the protein structure necessary to calculate $G^{\text{el}}(\text{P} + \text{L})$ in the TK description is the calcium loaded one, i.e., the protein in its holo form.

Assuming a homogeneous dielectric media, the TK equations are largely simplified.²⁰ For a protein containing N_p fixed charges, G^{el} is numerically equal to

$$G^{\text{el}} = -\frac{e^2}{8\pi\epsilon_0} \sum_{i=1}^{N_p} \sum_{j=1}^{N_p} z_i z_j (A_{ij} - C_{ij}) \quad (9)$$

with

$$A_{ij} = \frac{1}{\epsilon_s r_{ij}} \quad (10)$$

$$C_{ij} = \frac{1}{(R_p + R_s)\epsilon_s} \left[\frac{x}{1+x} + x^2 \sum_{n=1}^{\infty} \frac{2n+1}{2n-1} \left(\frac{\epsilon_s}{(2n+1)\epsilon_s} \right)^2 \left(\frac{r_i r_j}{(R_p + R_s)^2} \right)^n P_n(\cos \theta_{ij}) \right] \left/ \left(\frac{K_{n+1}(x)}{K_{n-1}(x)} \right) \right. \quad (11)$$

where

$$x = \kappa(R_p + R_s) \quad (12)$$

and

$$K_n(x) = \sum_{p=0}^n \left[\frac{\binom{n}{p}}{\binom{2n}{p}} \right] \frac{(2x)^p}{p!} \quad (13)$$

It is clear from eqs 9–13 that the salt screening effect is solely described by the C_{ij} terms through the κ parameter. This is the *key variable* in the physical description of electrolyte systems. In its standard formulation, the summation in eq 8 is only taken over the added salt particles. This means that κ is a function exclusively of the solution ionic strength, excluding the screening due to the presence of other charged species in the electrolyte solution. Therefore, the original TK model is mathematically not able to describe protein concentration effects since it was designed to describe just the salt screening.

In the colloidal literature, the concept of κ as a scaling parameter that measures the effectiveness of the Coulomb shielding has been revisited by different authors.^{24,73–76} As a parameter, the inclusion of other charged species is perfectly viable and adopted with success to describe the electrical interactions screening phenomena in concentrated colloidal systems.^{24,74,75} For instance, Beresford-Smith and co-workers^{73–75} considered it necessary to include the counterion concentration in the summation of eq 8 together with an electroneutrality condition that defines a new screening length definition (κ_c)

$$\kappa_c^{-1} = \left[\frac{\epsilon_0\epsilon_s k_B T}{1000e^2(n_{0,1}(z_1)^2 + n_{0,2}(z_2)^2)} \right]^{1/2} \quad (14)$$

where the subscript 1 and 2 of the species density and valency denote the counterions and coions, respectively.

Physically the situation is equivalent to invoke the so-called “effective charge” concept.⁷⁶ Around the protein charged surface there is a neutralizing counterion cloud that can be tightly bound near this surface. Therefore, other charged species at a separation distance of κ^{-1} apart from the protein surface will feel a smaller *effective* charge $Z_p^* = Z_p - N_c^*$, where N_c^* is the number of monovalent counterions present in the formed electrical double layer. This is similar to saying that κ^{-1} is the thickness of the neutralizing counterion cloud. A “total” screening length (κ_t) that accounts as well for the macromolecule concentration in the summation of eq 8 has been generalized as²⁴

$$\kappa_t^{-1} = \left[\frac{\epsilon_0\epsilon_s k_B T}{1000e^2(n_{0,0}(z_0)^2 + n_{0,1}(z_1)^2 + n_{0,2}(z_2)^2)} \right]^{1/2} \quad (15)$$

where the subscript 0 of the species density and valency denote the macromolecule and 1 and 2 have the same meanings as in eq 14. Perceive, however, that $n_{0,1}$ is defined as

$$n_{0,1} = -\frac{n_{0,0}z_0 + n_{0,2}z_2}{z_1} \quad (16)$$

due to the electroneutrality condition.⁷⁵

Incorporating these simple redefinitions of κ in eq 12 permits the description of the protein concentration effect. That is

$$x = \kappa_c(R_p + R_s) \quad (17)$$

and

$$x = \kappa_t(R_p + R_s) \quad (18)$$

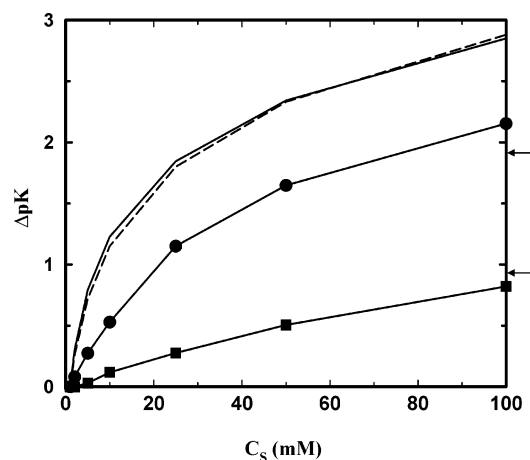


Figure 2. Total shift in the ion binding constant ΔpK at different macromolecular concentrations c_p are plotted as a function of salt concentration c_s for a protein model with a central net charge $Z_p = -8e$. A reference state at $c_s = 1$ mM is chosen, and the protein is allowed to bind two divalent cations. Results from the original TK and MC simulations data are compared as dashed and solid lines, respectively. Solid lines marked by filled circles correspond to $c_p = 0.2$ mM, and those marked by filled squares denote $c_p = 2$ mM, while unmarked lines refer to a $c_p = 20$ μ M. The arrows indicate the value of the modified TK schemes for the system at $c_p = 2$ mM. The upper and lower arrows correspond to TK_c and TK_t , respectively.

We shall refer to the resulting models as modified TK models (TK_c and TK_t), where the same subscripts adopted in eqs 17–18 are used to label them. Similar notation is followed for the pK shifts. Although the more critical case for the original TK scheme is at low salt and high protein concentrations, no difference between concentration regimes is observed when applying the new κ values. This is because the effect was found to be marginal for the noncritical cases. When adopting these new schemes, μ_F^{ex} should likewise reflect the proper macromolecular concentration. Consequently, eq 7 is rewritten in terms of κ_c and κ_t .

Results and Discussion

From a previous study,²⁰ it is known that pK shifts for calcium binding upon the addition of salt is well described by the TK description for moderately charged proteins at a low macromolecular concentration ($c_p = 20$ μ M). This is confirmed by the data shown in Figure 2. In this plot, salt pK shifts for a protein model with $Z_p = -8$ as a function of the ionic strength obtained from the MC simulations are given at different macromolecular concentrations. It can be observed that an increase in the protein concentration results in a considerable decrease in the ΔpK values caused by an increase in the Coulomb shielding. This is an effect that cannot be even qualitatively described in the original TK formulation since the results always reflect the infinite dilution regime. As a consequence, this limitation leads to a gradual departure of the TK results from the MC data, as seen in Figure 2. At a salt concentration close to physiological conditions, a macromolecular concentration 2 orders of magnitude higher than 20 μ M drops down the salt pK shifts to one-third of its value at the low concentration. Considering that a typical NMR experiment is carried out around 1 mM, this indicates a clear drawback of the original TK scheme that will become even more pronounced for a high protein charge. For instance, the same binding process for a protein with $Z_p = -24$ at $c_p = 2$ mM shows a large discrepancy of about $18k_B T$ units for the comparison between the ΔpK obtained from the simulations and the analytical theory. Conversely, the modified TK schemes (data indicated by the

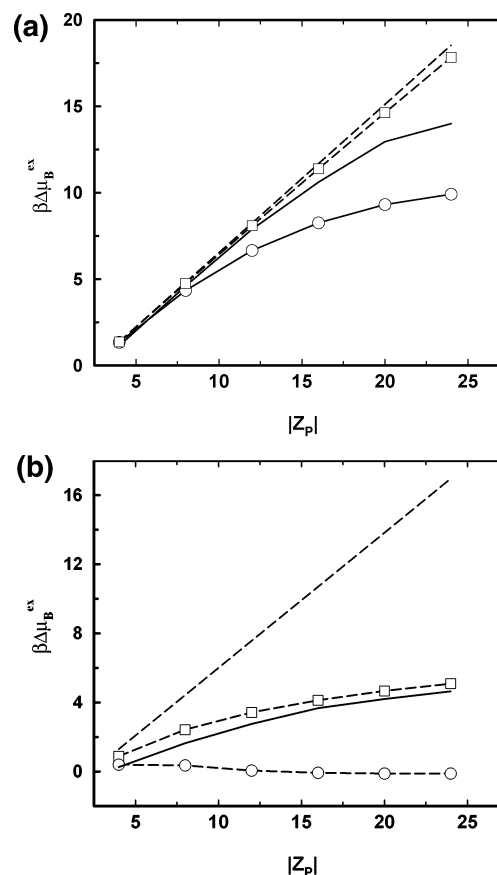


Figure 3. Differences of the excess chemical potentials $\beta\Delta\mu_B^{\text{ex}} = \beta\mu_B^{\text{ex}}(c_s) - \beta\mu_B^{\text{ex}}(c_s = 1 \text{ mM})$ at the binding sites for a divalent cation in a bulk monovalent electrolyte solution plotted as a function of the protein net charge (Z_p). A reference state at salt concentration $c_s = 1$ mM is chosen, and the final salt concentration is 100 mM. Results from MC simulations and the analytical schemes calculations are compared as solid and dashed lines, respectively. Lines marked by open squares correspond to TK_c , and those marked by open circles denote TK_t while unmarked lines refer to the original TK scheme. (a) System at low macromolecular concentration ($c_p = 20$ μ M). (b) System at typical NMR experimental conditions ($c_p = 2$ mM).

arrows in this graphic) are able to almost quantitatively reproduce the MC predictions. The found discrepancy is assumed to be small principally because these modified schemes are still neglecting nonlinear thermal effects and explicit ion–ion correlations.

Although the electrostatic free energy changes depend both on μ_B^{ex} and μ_F^{ex} , the former is responsible for larger contributions. Therefore, in Figure 3 we examine $\Delta\mu_B^{\text{ex}}$ as a function of the protein net charge in two different macromolecular concentration regimes. In both cases, the final salt concentration is 100 mM, and the reference state is at $c_s = 1$ mM. At low c_p (Figure 3a), the modified TK_c scheme produces almost the same outcomes as the original TK. For highly charged proteins ($Z_p > 12$), this analytical theory is not capable of accounting for the increase in the ion–ion correlations and the nonlinear effects despite the fact that the counterion screening is better described by the TK_c model. However, the TK_t overpredicts the Coulomb shielding due to a strong dependence with the square of the protein charge. In this description, even the counterion cloud of a modestly charged protein is assumed to tightly associate with its surface. Figure 3b shows the same data for $c_p = 2$ mM. In this case, the original TK model starts to break down already for a low macromolecular charge. For $Z_p = -8$, the difference between MC and TK data is about $2k_B T$. However, the inclusion

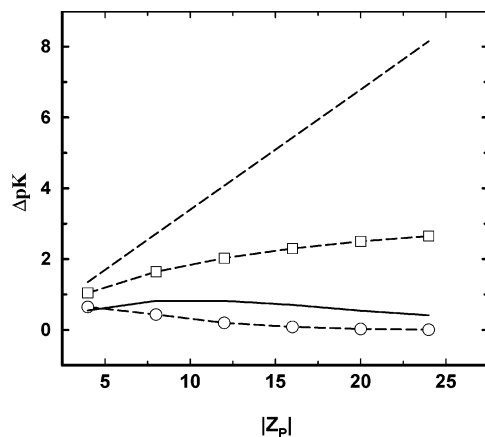


Figure 4. Total shift in the ion binding constant ΔpK , owing to solution ionic strength, plotted as a function of the protein net charge (Z_p). The protein concentration is $c_p = 2$ mM. Other details are as for Figure 3.

of the counterions in the summation of eq 8 starts to play a role already for a weakly charged protein. The linear behavior of the original TK scheme is lost, and the results approach the MC data regardless the protein net charge. The disagreement with MC simulation results is less than $1k_B T$ for almost all values of Z_p . Again, TK_t overscreened the macromolecular charge up to the situation that negative values of $\Delta\mu_B^{\text{ex}}$ are found for $|Z_p| > 8$.

A complementary picture of the behavior of the analytical descriptions taking into account both the μ_B^{ex} and μ_F^{ex} contributions is presented in Figure 4. The same trends already shown for μ_B^{ex} are repeated here. However, TK_t is more efficient than TK_c to recover the MC simulation data in this case. This is probably due to a cancellation of effects since both excess chemical potential expressions (eqs 7 and 9) are subjected to a large macromolecular screening when following the “total” screening length definition. As a matter of fact, μ_F^{ex} as defined by eq 7 is also not affected by the protein charge.

An important characteristic of the modified TK schemes is that they are able to confirm and describe the “protein concentration effect” on binding affinities.¹⁸ This is an important step forward since the ordinary TK model cannot predict pK shifts upon increase of protein concentration, as already mentioned. Calcium binding constants measured by Linse and coauthors using NMR spectroscopy for the N56A calbindin D_{9k} mutant at $c_p = 3.3$ mM¹⁸ were used to benchmark the new TK schemes suggested here. In all of the following calculations, the protein modeling was done by the all-atom model (model 2). Figure 5a shows the theoretical and experimental values assuming the system with no added salt as a reference. The overall agreement between the experimental data and the TK_c predictions is quite good. The level of agreement is surprising given that just a slight modification of κ was done in TK_c . These data thus confirm the importance of a proper description of the Coulomb shielding for electrostatic modeling. It is interesting to remark how close the TK_c and MC data are.

A final test is to compare the shifts at both high salt and protein concentrations. Figure 5b demonstrates the pK shifts at this extreme condition where the protein concentration was kept constant at $c_p = 3.3$ mM and the ionic strength was in the range of 0–1 M. All curves show at least a 3-fold reduction of ΔpK results in comparison to similar experiments carried out at low protein concentration⁷⁷ due to the high charge screening at this system condition. The peculiar invariable behavior of the experimental binding constants up to 50 mM of added salt is captured only by the MC simulations and partially by TK_t . The

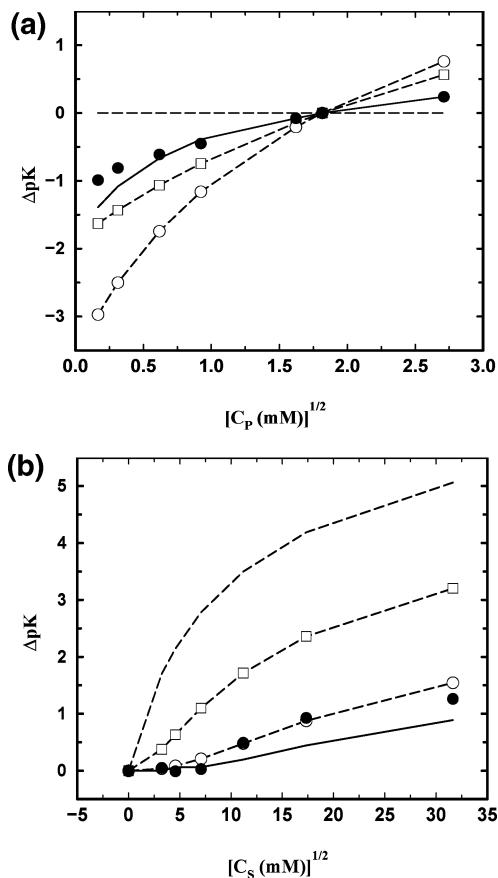


Figure 5. Shifts in binding constants for Ca^{2+} to N56A calbindin D_{9k} mutant. The macromolecule is described by the all-atom model in all these calculations. The experimental and MC data were taken from ref. 18. Filled circles are used to represent the experimental data. Other details are as for Figure 3. (a) pK shifts as a function of the macromolecular concentration. The salt concentration is fixed at $c_s = 0$ mM. A reference state at $c_p = 3.3$ mM is chosen. (b) pK shifts upon addition of salt for the system at $c_p = 3.3$ mM. The binding constant at 0 mM salt is taken as reference.

other benchmarked analytical scheme is not able to reproduce them. However, in general we find that the TK_t descriptions are closer to the experimental results than the other analytical scheme. The reason for that might be the strong screening characteristics of its formulation. Conversely, a further increase of the protein concentration distorts the present agreement. The large ΔpK values obtained by the original TK model clearly indicate a lack of a proper treatment of the Coulomb shielding. Comparing all TK schemes, one can easily see that macromolecular concentration does play a role in the binding process, and they all can describe such mechanism at least in a qualitative manner. A critical analysis of TK_c would suggest its wide implementation despite the differences found between the calculated and the experimental shifts. At the highest salt concentration, it predicts a ΔpK value that is off by less than one pK unit.

Similar qualitative data is obtained for the highly charged calmodulin ($Z_p = -24e$) as seen in Figure 6. With a null ionic strength, Figure 6 shows pK shifts upon an increase of calmodulin concentration, exclusively. The experimental protein concentration dependence is well reproduced by both new TK schemes (TK_c and TK_t). The TK model in its standard description is again not capable to describe even qualitatively such mechanism. The agreement between the theoretical data given by MC and TK_t with the experimental outcomes is good despite the fact that a rigid model is adopted for calmodulin. In

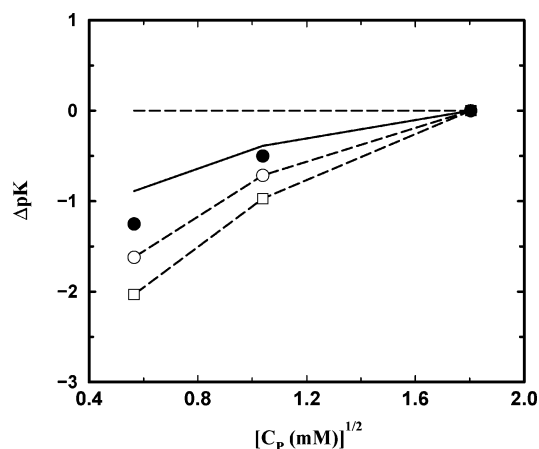


Figure 6. Shifts in binding constants for Ca^{2+} to calmodulin upon an increase of protein concentration. The salt concentration is fixed at $c_s = 0$ mM, while a reference state at $c_p = 3.25$ mM is chosen. Filled circles are used to represent the experimental data. All other details are as for Figure 5.

contrast with the calbindin case, TK_t does for this system a better job, which is probably related with the high charge of calmodulin and the way TK_t is defined. A high macromolecular charge dominates the screening parameter κ_t .

Concluding Remarks

The present work analyzes when and why the original TK approximation fails to describe ion binding affinities. It was demonstrated that the original TK model has a clear limitation to predict binding constants at moderate and high macromolecular concentrations. Although such a scheme correctly predicts salt shifts for weakly charged proteins at low protein concentration, modifications are necessary to properly capture the physics of the electrostatic screening under more general conditions. Two simple modified schemes were suggested based on different screening length definitions available in the colloidal literature. They keep the original TK simplicity and satisfactorily predict MC and experimental shifts in calcium binding constants as a function of protein concentration for calbindin $\text{D}_{9\text{k}}$ mutant and calmodulin. Due to their simplicity, they can be straightforwardly implemented in a large number of molecular modeling packages used to study the electrostatic biomolecular phenomena^{34,42–44,64,78–80} and also in closely related analytical theories such as the generalized Born theory.^{81,82} This will lead to an improve in their agreement between theoretical predictions with experimental data since the experiments are usually performed at high macromolecular concentrations. All theoretical calculations presented here did confirm the existence of the “protein concentration effect” as a phenomenon that results from a general electrostatic screening by the presence of other charged species.

Acknowledgment. This work has been supported in part by the Conselho Nacional de Desenvolvimento Científico e Tecnológico (CNPq) and Fundação de Amparo a Pesquisa do Estado de São Paulo (Fapesp) whom we thank. Computational resources were also provided in part by Cenapad/Brazil. It is also a pleasure to acknowledge fruitful discussions with Bo Jönsson and Márcia O. Fenley and their careful and critical reading of the manuscript.

References and Notes

(1) Perutz, M. F. Electrostatic effects in proteins. *Science* **1978**, *201*, 1187–1191.

(2) Warshel, A.; Russel, S. T.; Churg, A. K. Macroscopic models for studies of electrostatic interactions in proteins: Limitations and applicability. *Proc. Natl. Acad. Sci. U.S.A.* **1984**, *81*, 4785–4789.

(3) Matthew, J. B.; Gurd, F. R. N.; Garciamoreno, E. B.; Flanagan, M. A.; March, K. L.; Shire, S. J. pH dependent processes in proteins. *CRC Crit. Rev. Biochem.* **1985**, *18*, 91–197.

(4) Warshel, A.; Åqvist, J. Electrostatic energy and macromolecular function. *Annu. Rev. Biophys. Biophys. Chem.* **1991**, *20*, 267–298.

(5) Sharp, K. A.; Fine, R.; Honig, B. Computer simulations of the diffusion of a substrate to an active site of an enzyme. *Science* **1987**, *236*, 1460–1463.

(6) Nicholls, A.; Honig, B. Classical electrostatics in biology and chemistry. *Science* **1995**, *268*, 1144–1149.

(7) Fogolari, F.; Zuccato, P.; Esposito, G.; Viglino, P. Biomolecular electrostatics with the linearized Poisson–Boltzmann equation. *Biophys. J.* **1999**, *76*, 1–16.

(8) Fogolari, F.; Brigo, A.; Molinari, H. The Poisson–Boltzmann equation for biomolecular electrostatics: A tool for structural biology. *J. Mol. Recognit.* **2002**, *15*, 377–392.

(9) Gilson, M. K.; Honig, B. Calculation of electrostatic potentials in an enzyme active site. *Nature* **1987**, *330*, 84–86.

(10) Sternberg, M. J. E.; Hayes, F. R. F.; Russell, A. J.; Thomas, P. G.; Fersht, A. R. Prediction of electrostatic effects of engineering of protein charges. *Nature* **1997**, *330*, 86–88.

(11) Sheinerman, F. B.; Honig, B. On the role electrostatic interactions in the design of protein–protein interfaces. *J. Mol. Biol.* **2002**, *318*, 161–177.

(12) Zhou, H.-X.; Wong, K.-Y.; Vijayakumar, M. Design of fast enzymes by optimizing interaction potential in active site. *Proc. Natl. Acad. Sci. U.S.A.* **1997**, *94*, 12372–12377.

(13) Stigter, D.; Dill, K. A. Charge effects on folded and unfolded proteins. *Biochemistry* **1990**, *29*, 1262–1271.

(14) Northrup, S. H.; Wensel, T. G.; Meares, C. F.; Wendoloski, J. J.; Matthew, J. B. Electrostatic field around cytochrome c: Theory and energy transfer experiment. *Proc. Natl. Acad. Sci. U.S.A.* **1990**, *87*, 9503–9508.

(15) Archontis, G.; Simonson, T. Proton binding to proteins: A free-energy component analysis using a dielectric continuum model. *Biophys. J.* **2005**, *88*, 3888–3904.

(16) Garcia-Moreno, B. Probing structural and physical basis of protein energetics linked to protons salt. *Methods Enzymol.* **1995**, *259*, 512–538.

(17) Svensson, B.; Jönsson, B.; Thulin, E.; Woodward, C. Binding of Ca^{2+} to calmodulin and its tryptic fragments: Theory and experiment. *Biochemistry* **1993**, *32*, 2828–2834.

(18) Linse, S.; Jönsson, B.; Chazin, W. J. The effect of protein concentration on ion binding. *Proc. Natl. Acad. Sci. U.S.A.* **1995**, *92*, 4748–4752.

(19) Padmanabhan, S.; Zhang, W.; Capp, M. W.; Anderson, C. F.; Record, M. T., Jr. Binding of cationic (+4) alanine- and glycine-containing oligopeptides to double-stranded DNA: Thermodynamic analysis of effects of Coulombic interactions and α -helix induction. *Biochemistry* **1997**, *36*, 5193–5206.

(20) da Silva, F. L. B.; Jönsson, B.; Penfold, R. A critical investigation of the Tanford–Kirkwood scheme by means of Monte Carlo simulations. *Protein Sci.* **2001**, *10*, 1415–1425.

(21) de Kruijff, C. G.; Weinbreck, F.; de Vries, R. Complex coacervation of proteins and anionic polysaccharides. *Curr. Opin. Colloid. Interface Sci.* **2004**, *9*, 340–349.

(22) da Silva, F. L. B.; Linse, S.; Jönsson, B. Binding of charged ligands to macromolecules. Anomalous salt dependence. *J. Phys. Chem. B* **2005**, *109*, 2007–2013.

(23) da Silva, F. L. B.; Lund, M.; Jönsson, B.; Åkesson, T. On the interaction between protein and polyelectrolyte. *J. Phys. Chem. B*, **2006**, *110*, 4459–4464.

(24) Lin, S.-C.; Lee, W. I.; Shurr, J. M. Brownian motion of highly charged poly(L-lysine). Effects of salt and polyion concentration. *Biopolymers* **1978**, *17*, 1041–1064.

(25) Spolar, R. S.; Record, M. T., Jr. Coupling of local folding to site-specific binding of proteins to DNA. *Science* **1994**, *263*, 777–784.

(26) Lodish, H.; Berk, A.; Zipursky, S. L.; Matsudaira, P.; Baltimore, D.; Darnell, J. E. *Molecular Cell Biology*, 4th ed.; W. H. Freeman & Company: New York, 1999.

(27) Wider, G. Structure determination of biological macromolecules in solution using NMR spectroscopy. *BioTechniques* **2000**, *29*, 1278–1294.

(28) Hill, T. L. *Statistical Mechanics*; McGraw-Hill: New York, 1956.

(29) Linderström-Lang, K. Om proteinstoffernes ionisation. *C. R. Trav. Lab. Carlsberg* **1924**, *15*, 1–28.

(30) Fogolari, F.; Ragona, L.; Licciardi, S.; Romagnoli, S.; Michelutti, R.; Ugnolini, R.; Molinari, H. Electrostatic properties of bovine β -lactoglobulin. *Proteins: Struct., Funct., Genet.* **2000**, *39*, 317–330.

(31) Bashford, D.; Karplus, M. pK_a 's of ionizable groups in proteins: Atomic detail from a continuum electrostatic model. *Biochemistry* **1990**, *29*, 10219–10225.

- (32) Juffer, A. H. Theoretical calculations of acid-dissociation constants of proteins. *Biochem. Cell Biol.* **1998**, *76*, 198–209.
- (33) Havranek, J. J.; Harbury, P. B. Tanford–Kirkwood electrostatics for protein modeling. *Proc. Natl. Acad. Sci. U.S.A.* **1999**, *96*, 11145–11150.
- (34) Boschitsch, A. H.; Fenley, M. O. Hybrid boundary element and finite difference method for solving the nonlinear Poisson–Boltzmann equation. *J. Comput. Chem.* **2004**, *25*, 935–955.
- (35) Warwicker, J.; Watson, H. C. Calculation of the electric potential in the active site cleft due to α -helix dipoles. *J. Mol. Biol.* **1982**, *157*, 671–679.
- (36) Tanford, C.; Kirkwood, J. G. Theory of protein titration curves I. General equations for impenetrable spheres. *J. Am. Chem. Soc.* **1957**, *79*, 5333–5339.
- (37) Fushiki, M.; Svensson, B.; Jönsson, B.; Woodward, C. E. Electrostatic interactions in protein solution—A comparison between Poisson–Boltzmann and Monte Carlo calculations. *Biopolymers* **1991**, *31*, 1149–1158.
- (38) Kesvatera, T.; Jönsson, B.; Thulin, E.; Linse, S. Focusing of the electrostatic potential at EF-hands of calbindin D_{9k}: Titration of acidic residues. *Proteins: Struct., Funct., Genet.* **2001**, *45*, 129–135.
- (39) Degreve, L.; da Silva, F. L. B. Detailed study of 1 M aqueous NaCl solution by computer simulations. *J. Chem. Phys.* **1999**, *111*, 5150–5156.
- (40) Frenkel, D.; Smit, B. *Understanding Molecular Simulation: From Algorithms to Applications*; Academic Press: San Diego, CA, 1996.
- (41) Lazaridis, T.; Karplus, M. Effective energy functions for protein structure prediction. *Curr. Opin. Struct. Biol.* **2000**, *10*, 139–145.
- (42) Sharp, K. A.; Nicholls, A.; Sridharan, S. *Delphi—A Macromolecular Electrostatics Modeling Package*; Columbia University: New York, 1998.
- (43) Bashford, D.; Gerwert, K. Electrostatic calculations of the pK_a values of ionizable groups in bacteriorhodopsin. *J. Mol. Biol.* **1992**, *224*, 473–486.
- (44) Davis, M. E.; Madura, J. D.; Luty, B. A.; McCammon, J. A. Electrostatics and diffusion of molecules in solution—Simulations with the University of Houston Brownian dynamics program. *Comput. Phys. Commun.* **1991**, *62*, 187–197.
- (45) Berman, H. M.; Westbrook, J.; Feng, Z.; Gilliland, G.; Bhat, T. N.; Weissig, H.; Shindyalov, I. N.; Bourne, P. E. The Protein Data Bank. *Nucleic Acids Res.* **2000**, *28*, 235–242.
- (46) *Protein Data Bank*, 2005. <http://www.rcsb.org/pdb>.
- (47) Linse, S.; Brodin, P.; Johansson, C.; Thulin, E.; Grundström, T.; Forsen, S. The role of protein surface changes in ion binding. *Nature* **1988**, *335*, 651–652.
- (48) Szebenyi, D. M. E.; Moffat, K. The refined structure of vitamin D-dependent calcium-binding protein from bovine intestine. Molecular details, ion binding, and implications for the structure of other calcium-binding proteins. *J. Biol. Chem.* **1986**, *261*, 8761–8777.
- (49) Babu, Y. S.; Bugg, C. E.; Cook, W. J. Structure of calmodulin refined at 2.2 Å resolution. *J. Mol. Biol.* **1988**, *204*, 191–204.
- (50) Levesque, D.; Weis, J. J.; Hansen, J. P. Simulation of classical fluids. In *Monte Carlo Methods in Statistical Physics*; Binder, K., Ed.; Springer-Verlag: Berlin, 1986; Vol. 5, pp 47–119.
- (51) Harvey, S. C. Treatment of electrostatic effects in macromolecular modeling. *Proteins: Struct., Funct., Genet.* **1989**, *5*, 78–92.
- (52) Bashford, D. Electrostatic effects in biological molecules. *Curr. Opin. Struct. Biol.* **1991**, *1*, 175–184.
- (53) Sharp, K. A. Electrostatic interactions in macromolecules. *Curr. Opin. Struct. Biol.* **1994**, *4*, 234–239.
- (54) Antonsiewicz, J.; McCammon, J. A.; Gilson, M. K. The determinants of pK_as in proteins. *Biochemistry* **1994**, *35*, 7819–7833.
- (55) Simonson, T.; Brooks, C. L., III. Charge screening and the dielectric constant of proteins: Insights from molecular dynamics. *J. Am. Chem. Soc.* **1996**, *118*, 8452–8458.
- (56) Löffler, G.; Sreiber, H.; Steinhauser, O. Calculation of the dielectric properties of a protein and its solvent: Theory and a case study. *J. Mol. Biol.* **1997**, *270*, 520–534.
- (57) Warwicker, J.; Simplied methods for pK_a acid pH dependent stability estimation in proteins: Removing dielectric and counterion boundaries. *Protein Sci.* **1999**, *8*, 418–425.
- (58) Juffer, A. H.; Vogel, H. J. pK_a calculations of calbindin D_{9k}: Effects of Ca²⁺ binding, protein dielectric constant, and ionic strength. *Proteins* **2000**, *41*, 554–567.
- (59) Kesvatera, T.; Jönsson, B.; Thulin, E.; Linse, S. Ionization behavior of acidic residues in calbindin D_{9k}. *Proteins: Struct., Funct., Genet.* **1999**, *37*, 106–115.
- (60) Svensson, B.; Jönsson, B.; Woodward, C. E.; Linse, S. Ion binding properties of calbindin D_{9k}—A Monte Carlo simulation study. *Biochemistry* **1991**, *30*, 5209–5217.
- (61) Baptista, A. M.; Soares, C. M. Some theoretical and computational aspects of the inclusion of proton isomerism in the protonation equilibrium of proteins. *J. Phys. Chem. B* **2001**, *105*, 293–309.
- (62) Lund, M.; Jönsson, B. On the charge regulation of proteins. *Biochemistry* **2005**, *44*, 5722–5727.
- (63) Spassov, V.; Bashford, D. Electrostatic coupling to pH-titrating sites as a source of cooperativity in protein–ligand binding. *Protein Sci.* **1998**, *7*, 2012–2025.
- (64) Jönsson, B. The Thermodynamics of Ionic Amphiphile–Water Systems: A Theoretical Analysis. Ph.D. Thesis, Lund University, Lund, Sweden, 1981.
- (65) Marcus, R. A. Calculation of thermodynamic properties of poly-electrolytes. *J. Chem. Phys.* **1955**, *23*, 1057.
- (66) da Silva, F. L. B.; Bogren, D.; Söderman, O.; Jönsson, B. Titration of fatty acids solubilized in cationic, nonionic and anionic micelles: Theory and experiment. *J. Phys. Chem. B* **2003**, *106*, 3515–3522.
- (67) Metropolis, N. A.; Rosenbluth, A. W.; Rosenbluth, M. N.; Teller, A.; Teller, E. Equation of state calculations by fast computing machines. *J. Chem. Phys.* **1953**, *21*, 1087–1097.
- (68) Svensson, B.; Jönsson, B.; Fushiki, M.; Linse, S. Ionic strength effects on the binding constant of calcium chelators—Experiment and theory. *J. Phys. Chem.* **1992**, *96*, 3135–3138.
- (69) Widom, B. Some topics in the theory of fluids. *J. Chem. Phys.* **1963**, *39*, 2808–2812.
- (70) Svensson, B. R.; Woodward, C. E. Widom’s method for uniform and non-uniform electrolyte solutions. *Mol. Phys.* **1988**, *64*, 247–259.
- (71) Penfold, R.; Warwicker, J.; Jönsson, B. Electrostatic models for calcium binding proteins. *J. Phys. Chem. B* **1998**, *108*, 8599–8610.
- (72) Hill, T. L. *An Introduction to Statistical Thermodynamics*; Dover Publications: New York, 1986.
- (73) Beresford-Smith, B. Some Aspects of Strongly Interacting Colloidal Dispersions. Ph.D. Thesis, Australian National University, Canberra, 1985.
- (74) Beresford-Smith, B.; Chan, D. Y. C. Electrical double layer interactions in concentrated colloidal systems. *Faraday Discuss. Chem. Soc.* **1983**, *76*, 65–75.
- (75) *Macro-Ion Characterization: From Dilute Solutions to Complex Fluids*; Schmitz, K. S., Ed.; ACS Symposium Series 548; American Chemical Society: Washington, DC, 1994.
- (76) Kjellander, R.; Ulander, J. Effective ionic charges, permittivity and screening length: Dressed ion theory applied to 1:2 electrolyte solutions. *Mol. Phys.* **1996**, *95*, 495–505.
- (77) Kesvatera, T.; Jönsson, B.; Thulin, E.; Linse, S. Binding of Ca²⁺ to calbindin D_{9k}: Structural stability and function at high salt concentration. *Biochemistry* **1996**, *33*, 14170–14176.
- (78) Holst, M.; Baker, N.; Wang, F. Adaptive multilevel finite element solution of the Poisson–Boltzmann equation I. Algorithms and examples. *J. Comput. Chem.* **2000**, *21*, 1319–1342.
- (79) Juffer, A. H. *Mel—The Macromolecular Electrostatics Computer Program*; Laboratory of Physical Chemistry, University of Groningen: Groningen, The Netherlands, 1992.
- (80) Boschitsch, A. H.; Fenley, M. O.; Zhou, H. X. Fast boundary element method for the linear Poisson–Boltzmann equation. *J. Phys. Chem. B* **2001**, *106*, 2741–2754.
- (81) Bashford, D.; Case, D. A. Generalized born models of macromolecular solvation effects. *Annu. Rev. Phys. Chem.* **2000**, *51*, 129–152.
- (82) Onufriev, A.; Bashford, D.; Case, D. A. Exploring protein native states and large-scale conformational changes with a modified generalized Born model. *Proteins: Struct., Funct., Bioinf.* **2004**, *55*, 383–394.